J. Astron. Space Sci. 23(1), 1–10 (2006)

BVR PHOTOMETRY OF SUPERGIANT STARS IN HOLMBERG II[1]

Y.-J. Sohn†, S.-W. Chang, D.-Y. Kim, J.-W. Kim, S.-H. Kim, J.-E. Lee, J. G. Lee, J.-M. Lee, M.-Y. Lee, S.-Y. Lee, U.-S. Lee, B.-K. Park, H.-E. Park, I.-K. Park, W. H. Park, H.-S. Yi, and J.-Y. Yoon

Department of Astronomy, Yonsei University, Seoul 120-749, Korea

email: sohnyj@yonsei.ac.kr

(Received January 2, 2006; Accepted January 27, 2006)

ABSTRACT

We report the photometric properties in BVR bands for the resolved bright supergiant stars in the dwarf galaxy Holmberg II. The color-magnitude diagrams and color-color diagram of 374 resolved stars indicate that the majority of the member stars are supergiant stars with a wide range of spectral type between B-K. A comparison with theoretical evolutionary tracks indicates that the supergiant stars in the observed field have progenitor masses between $\sim 10M_{\odot}$ and $20M_{\odot}$. The exponent of luminosity function in V is in good agreement with those of the Small and Large Magellanic Clouds.

Keywords: photometry, supergiant stars, dwarf galaxy: Holmberg II

1. INTRODUCTION

Dwarf galaxies are the major constituent in the build-up of galaxy group and cluster (Gallagher & Wyse 1994, Grebel 1998, 2005, Grebel & Brandner 1999, van den Bergh 1999, Tolstoy 2003). Therefore, photometric stellar population study of dwarf galaxies can provide an important insight into the environmental condition of star formation and stellar evolution in the parent system. However, only the brightest stars can be resolved in nearby dwarf galaxies due to the low luminosity and small size of the systems. Meanwhile, photometric studies of supergiant stars, as the brightest stellar population in a galaxy, indeed provide a direct means of probing the recent star forming history of a galaxy (e.g. Sohn & Davidge 1996a,b, 1998). Studies of supergiant stars in a galaxy also provide a means of testing models of massive star evolution (e.g. Salasnich et al. 2000) and a potentially powerful means of measuring distance over cosmologically interesting scales (e.g. Rozanski & Rowan-Robinson 1994).

In this paper, we use B, V and R CCD images to investigate the supergiant contents of the dwarf irregular galaxy Holmberg II. Holmberg II (= DDO50 = UGC 4305) has long been considered to be a member of the M81 group of galaxies as a Magellanic type irregular galaxy (de Vaucouleurs 1964). The NED database provides an apparent size to be about $7'.9 \times 6'.3$ with a total magnitude

[1]Based on observations carried out at the BOAO 1.8m telescope, operated by the Korea Astronomy and Space Science Institute.

†corresponding author

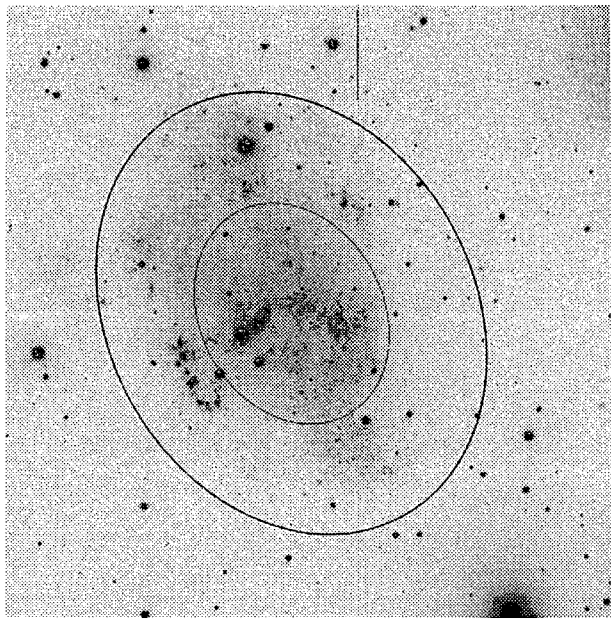

Figure 1. Flat-fielded image of Holmberg II in B band and the selected ellipse regions. The entire field-of-view is 10.43 × 10.43 arcmin^2.

of 11.10 mag in B. Holmberg II is one of the best studied object for the high rate of current star formation from the observations based on optical band (e.g. Hoessel & Danielson 1984) and the other bands such as FUV and HI (e.g. Stewart et al. 2000). Numerous holes are visible in the HI distributions of Holmberg II, surrounded by high density shells. Puche et al. (1992) identified 51 holes and showed that in many cases expansion of the gas surrounding the holes is directly detectable. Indeed, high spatial and spectral resolution observations of the neutral hydrogen gas in nearby dwarf and Magellanic irregular galaxies have revealed remarkably intricate and complex structures (Puche et al. 1992, Staveley-Smith et al. 1997, Kim et al. 1998). Using the P-L relation obtained from 28 Cepheid candidates, Hoessel et al. (1998) estimated a distance of 3.05 Mpc and the distance modulus of 27.42. The NED database provides the radial velocity of Holmberg II as 142 km/s and a redshift as 0.000474.

The observation, data reduction, and standardization procedure are described in Sec. 2. In Sec. 3, we present the color-magnitude diagrams (CMDs) and a color-color diagram of resolved stars in Holmberg II. We derive the mass range of supergiant stars by comparing with the theoretical massive star evolution tracks, and the luminosity functions of the resolved stars in Sec. 3. Results are summarized in Sec. 4.

2. OBSERVATION, DATA REDUCTION, AND STANDARDIZATION

B, V and R images of Holmberg II were obtained over the night in UT 2001 January 30 using the 1.8m telescope at BOAO. The detector was STIe CCD chip of 2048 × 2048 format. At the f/8

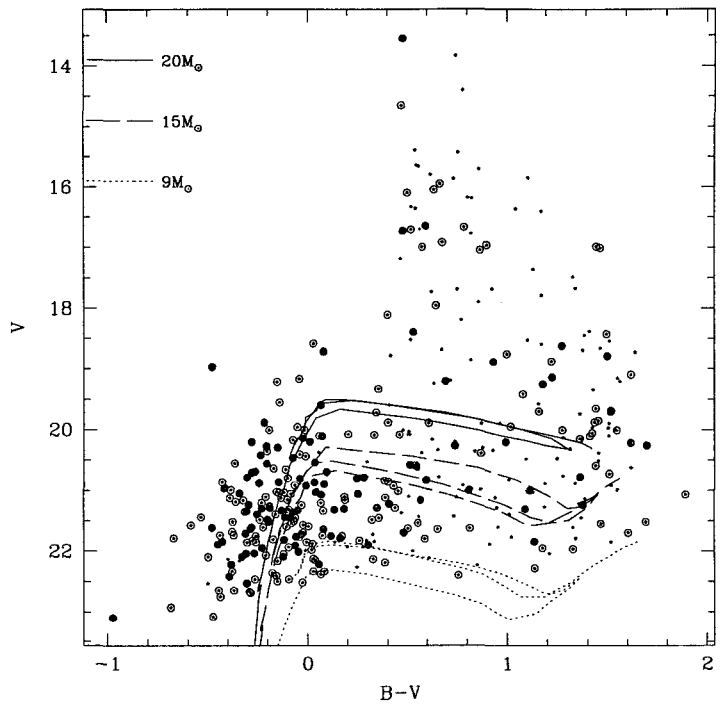

Figure 2. $(B-V, V)$ CMD of stars in Holmberg II. The dots indicate all stars detected in the observed field, open and closed circles show stars located in the outer ellipse and the inner ellipse, respectively. Solid, dashed and dotted lines are evolution tracks of stars with 20, 15 and $9M_{\odot}$.

Cassegrain focus, the image scale is 0.34 arcsec/pixel, which gives the sky coverage of 11.8×11.8 arcmin^2. A single exposure centered on the galaxy was taken in each filter with the exposure times of 1,500, 1,200 and 900 seconds in B, V and R, respectively. The seeings measured from the reduced images are 1.8, 1.7 and 1.5 arcsec FWHM in B, V and R, respectively.

The raw images were reduced using standard CCD processing techniques. A median bias frame was subtracted from the raw exposures, and the results were divided by sky-flats to remove additional pixel-to-pixel variation through the frame. The edge of the image was trimmed so as to consider stars at the 10.43×10.43 arcmin^2 area centered on Holmberg II. The flat-fielded image of Holmberg II in B is shown in Figure 1.

Observations were also made of a number of standard stars on the Landolt (1992) fields to derive the photometric standardization. Extinction coefficients were estimated from the data of time series observations of an arbitrary sky field through the run. The final photometric transformations are $V - v_o = -0.115(\pm 0.167)(b-v)_o - 1.392(\pm 0.218)$, $(B-V) = 1.245(\pm 0.115)(b-v)_o - 0.558(\pm 0.149)$, and $(V-R) = 0.684(\pm 0.170)(v-r)_o + 0.159(\pm 0.120)$.

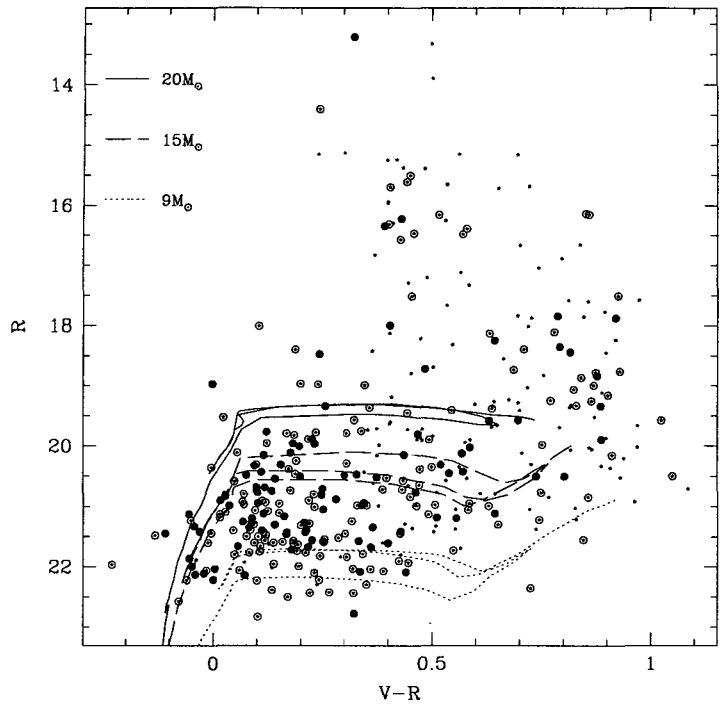

Figure 3. $(V-R, R)$ CMD of stars in Holmberg II. Symbols are the same as Figure 2.

3. PHOTOMETRIC PROPERTY

3.1 PHOTOMETRY

The brightness of individual stars were measured with the PSF-fitting program DAOPHOT II and ALLSTAR packages (Stetson 1987, Stetson & Harris 1988). A complicating factor is that unresolved stars and localized areas of high extinction conspire to create a nonuniform background in the plane of Holmberg II. This component was removed using an iterative approach (Sohn & Davidge 1996a): A preliminary set of stellar brightness were estimated from the original frames using DAOPHOT, and detected stars were then subtracted from the original data. A boxcar median filter with side dimension ~ 5 times the FWHM of the PSF was then applied to the residual image to remove artifacts of the star subtraction process and also to suppress any faint stars that may have fallen slightly below the limit of detection. These smoothed background images were then subtracted from the original data frames, and DAOPHOT and ALLSTAR were re-run on the results. Finally, total 374 stars are detected in all three bands of B, V and R. Table 1 lists the magnitude and colors of the resolved stars in Holmberg II.

3.2 COLOR-MAGNITUDE DIAGRAM AND COLOR-COLOR DIAGRAM

Figures 2 and 3 show the $(B-V, V)$ and $(V-R, R)$ CMDs of resolved stars in Holmberg

Table 1. Photometric properties of 374 detected stars in Holmberg II.

V	σ_V	$B-V$	$\sigma_{(B-V)}$	$V-R$	$\sigma_{(V-R)}$	V	σ_V	$B-V$	σ_{B-V}	$V-R$	$\sigma_{(V-R)}$
13.54	0.02	0.48	0.02	0.32	0.05	21.15	0.05	-0.10	0.06	0.01	0.08
14.65	0.01	0.47	0.01	0.24	0.03	21.15	0.05	0.19	0.07	0.43	0.06
15.95	0.00	0.67	0.00	0.45	0.00	21.16	0.06	-0.32	0.08	0.09	0.10
16.05	0.00	0.64	0.01	0.44	0.00	21.16	0.07	0.57	0.11	0.28	0.10
16.09	0.01	0.50	0.01	0.40	0.01	21.18	0.07	-0.36	0.09	-0.05	0.12
16.65	0.01	0.59	0.01	0.43	0.01	21.20	0.05	-0.23	0.07	0.01	0.08
16.67	0.00	0.78	0.01	0.51	0.00	21.20	0.05	0.07	0.07	0.12	0.08
16.71	0.00	0.52	0.01	0.40	0.01	21.22	0.05	0.41	0.07	0.46	0.07
16.73	0.00	0.48	0.01	0.39	0.01	21.23	0.05	-0.29	0.06	0.11	0.09
16.92	0.01	0.68	0.01	0.46	0.01	21.24	0.07	-0.03	0.09	0.23	0.17
16.96	0.00	0.90	0.01	0.58	0.01	21.24	0.05	1.38	0.13	0.74	0.07
16.99	0.03	1.45	0.04	0.85	0.06	21.26	0.05	-0.19	0.07	0.15	0.10
16.99	0.00	0.58	0.01	0.43	0.01	21.28	0.07	-0.19	0.09	0.09	0.11
17.01	0.01	1.47	0.01	0.86	0.01	21.28	0.05	0.35	0.09	0.34	0.08
17.04	0.00	0.86	0.01	0.57	0.00	21.29	0.05	0.44	0.08	0.45	0.07
17.96	0.01	0.64	0.01	0.45	0.01	21.29	0.07	-0.23	0.08	-0.04	0.11
18.11	0.03	0.40	0.05	0.10	0.05	21.30	0.05	0.18	0.07	0.25	0.08
18.40	0.01	0.53	0.01	0.40	0.01	21.30	0.06	1.09	0.13	0.80	0.07
18.43	0.01	1.50	0.02	0.92	0.01	21.31	0.06	-0.09	0.07	0.33	0.08
18.58	0.05	0.03	0.07	0.19	0.07	21.31	0.08	0.14	0.10	0.34	0.10
18.63	0.01	1.27	0.02	0.79	0.01	21.32	0.07	-0.05	0.08	0.07	0.10
18.71	0.01	0.08	0.02	0.24	0.02	21.32	0.06	-0.13	0.07	0.16	0.09
18.76	0.01	1.00	0.02	0.63	0.01	21.33	0.05	0.08	0.07	0.35	0.08
18.79	0.01	1.50	0.02	0.92	0.01	21.34	0.06	-0.31	0.08	-0.11	0.12
18.88	0.01	1.22	0.02	0.78	0.01	21.35	0.06	-0.31	0.08	-0.13	0.11
18.89	0.01	0.93	0.02	0.64	0.02	21.36	0.05	-0.07	0.08	0.09	0.09
18.97	0.03	-0.48	0.05	0.00	0.04	21.39	0.06	-0.25	0.08	-0.03	0.11
19.10	0.03	1.62	0.05	0.71	0.05	21.39	0.06	-0.16	0.08	0.09	0.11
19.14	0.01	1.22	0.02	0.79	0.01	21.43	0.06	-0.11	0.08	0.08	0.11
19.16	0.02	-0.04	0.03	0.20	0.03	21.44	0.06	-0.53	0.07	-0.01	0.11
19.20	0.02	0.69	0.03	0.48	0.03	21.44	0.06	-0.09	0.09	0.14	0.11
19.21	0.02	-0.15	0.03	0.24	0.02	21.45	0.06	-0.06	0.08	0.05	0.12
19.25	0.01	1.18	0.03	0.81	0.02	21.45	0.07	0.36	0.10	0.46	0.09
19.33	0.01	0.35	0.02	0.35	0.02	21.47	0.07	-0.20	0.09	0.21	0.11
19.42	0.01	1.08	0.03	0.68	0.02	21.48	0.06	-0.24	0.08	0.08	0.10
19.55	0.05	-0.14	0.07	0.02	0.08	21.48	0.07	0.32	0.10	0.51	0.09
19.59	0.03	0.07	0.05	0.25	0.05	21.50	0.07	-0.07	0.09	0.22	0.10
19.65	0.02	1.44	0.04	0.87	0.02	21.51	0.06	-0.19	0.08	0.11	0.12
19.69	0.02	1.52	0.04	0.93	0.02	21.51	0.05	-0.38	0.07	0.20	0.08
19.70	0.02	1.16	0.04	0.84	0.02	21.52	0.07	1.69	0.20	0.75	0.09
19.71	0.02	1.52	0.04	0.88	0.02	21.53	0.06	-0.08	0.08	0.11	0.09
19.72	0.02	0.34	0.02	0.36	0.02	21.54	0.07	0.55	0.11	0.58	0.10
19.86	0.02	1.45	0.04	0.87	0.02	21.55	0.07	1.47	0.19	1.05	0.08
19.88	0.02	-0.22	0.03	0.12	0.04	21.56	0.07	-0.02	0.09	0.32	0.10
19.88	0.02	1.43	0.05	0.82	0.03	21.57	0.08	-0.58	0.09	0.08	0.13
19.89	0.02	0.40	0.02	0.32	0.03	21.59	0.08	0.01	0.10	-0.01	0.14
19.89	0.02	0.61	0.03	0.44	0.02	21.59	0.07	-0.11	0.08	0.12	0.11
19.95	0.04	1.02	0.06	0.54	0.05	21.60	0.08	-0.28	0.09	0.17	0.11
19.95	0.02	-0.05	0.02	0.17	0.03	21.60	0.05	-0.22	0.07	0.10	0.12
20.00	0.04	-0.19	0.06	0.18	0.06	21.61	0.08	-0.48	0.10	0.21	0.12
20.00	0.03	-0.02	0.05	0.23	0.05	21.62	0.08	0.81	0.13	0.63	0.11
20.01	0.03	1.27	0.05	0.64	0.03	21.62	0.07	0.50	0.11	0.49	0.10
20.01	0.02	1.55	0.05	0.77	0.03	21.63	0.07	-0.29	0.09	0.17	0.10
20.06	0.02	1.42	0.06	0.90	0.03	21.64	0.06	0.08	0.09	0.21	0.09
20.08	0.05	0.20	0.07	0.12	0.08	21.64	0.07	0.65	0.13	0.58	0.11
20.08	0.02	0.46	0.03	0.34	0.03	21.68	0.08	-0.38	0.09	0.12	0.13
20.09	0.04	0.33	0.06	0.30	0.08	21.70	0.07	-0.02	0.09	0.09	0.12
20.10	0.02	0.06	0.03	0.22	0.03	21.70	0.09	0.48	0.12	0.51	0.11
20.11	0.02	0.07	0.03	0.22	0.03	21.70	0.10	1.60	0.22	0.86	0.11
20.11	0.02	1.41	0.06	0.86	0.03	21.71	0.08	-0.31	0.10	0.37	0.11
20.14	0.03	-0.02	0.04	0.18	0.04	21.72	0.07	-0.03	0.09	0.06	0.13
20.15	0.02	1.36	0.06	0.83	0.02	21.74	0.09	-0.37	0.11	-0.23	0.16
20.17	0.04	-0.07	0.05	0.06	0.06	21.74	0.08	-0.44	0.09	0.14	0.12
20.19	0.04	0.01	0.05	0.23	0.06	21.74	0.07	0.08	0.10	0.16	0.13
20.20	0.03	-0.28	0.04	0.20	0.04	21.75	0.07	-0.26	0.09	0.18	0.12
20.20	0.03	0.99	0.06	0.63	0.04	21.75	0.10	0.12	0.14	0.56	0.12
20.22	0.03	1.62	0.07	0.88	0.03	21.75	0.07	0.17	0.10	0.30	0.10
20.26	0.04	1.70	0.08	0.70	0.06	21.76	0.07	-0.06	0.09	0.64	0.09
20.26	0.03	0.74	0.05	0.47	0.04	21.76	0.06	-0.04	0.09	0.11	0.13
20.27	0.03	-0.21	0.03	0.12	0.04	21.78	0.10	0.16	0.15	0.22	0.14
20.29	0.04	-0.15	0.06	0.18	0.05	21.79	0.09	-0.67	0.10	0.18	0.14
20.35	0.04	-0.20	0.05	0.00	0.06	21.80	0.08	0.59	0.14	0.25	0.14

Table 1. (Continued)

V	σ_V	$B-V$	$\sigma_{(B-V)}$	$V-R$	$\sigma_{(V-R)}$	V	σ_V	$B-V$	σ_{B-V}	$V-R$	$\sigma_{(V-R)}$
20.39	0.05	0.87	0.07	0.49	0.06	21.80	0.10	-0.17	0.12	0.29	0.14
20.40	0.03	-0.04	0.04	0.10	0.04	21.81	0.08	-0.12	0.11	-0.05	0.16
20.42	0.04	-0.24	0.05	0.09	0.07	21.82	0.08	-0.28	0.11	0.19	0.12
20.43	0.03	-0.01	0.04	0.19	0.04	21.83	0.08	0.26	0.11	0.25	0.13
20.46	0.03	-0.08	0.04	0.15	0.05	21.84	0.08	-0.43	0.10	0.25	0.11
20.54	0.03	0.04	0.04	0.11	0.05	21.84	0.10	1.13	0.20	0.43	0.13
20.55	0.04	-0.37	0.04	0.17	0.05	21.85	0.07	0.00	0.10	0.05	0.15
20.56	0.03	-0.21	0.04	0.08	0.05	21.85	0.07	-0.26	0.10	0.08	0.16
20.58	0.03	0.51	0.05	0.44	0.04	21.86	0.08	-0.30	0.09	0.11	0.13
20.59	0.03	0.54	0.05	0.31	0.05	21.87	0.07	0.02	0.11	0.43	0.11
20.60	0.03	1.44	0.08	1.02	0.04	21.89	0.08	-0.45	0.11	0.22	0.13
20.61	0.04	0.55	0.06	0.59	0.04	21.90	0.09	0.30	0.14	0.18	0.14
20.63	0.04	-0.17	0.05	0.05	0.06	21.90	0.09	-0.06	0.12	0.33	0.13
20.65	0.04	-0.11	0.04	0.19	0.06	21.93	0.09	-0.09	0.12	0.19	0.13
20.69	0.04	-0.26	0.06	0.14	0.07	21.95	0.08	-0.23	0.12	-0.05	0.16
20.69	0.04	0.09	0.06	0.57	0.05	21.95	0.08	1.18	0.21	0.65	0.11
20.70	0.04	-0.28	0.05	0.20	0.06	21.97	0.10	1.33	0.25	0.74	0.13
20.73	0.05	1.51	0.11	0.75	0.07	21.98	0.08	0.02	0.11	0.21	0.15
20.78	0.05	1.36	0.10	0.89	0.05	22.00	0.11	-0.05	0.13	0.40	0.16
20.78	0.04	-0.31	0.05	0.10	0.06	22.03	0.11	-0.27	0.13	0.36	0.14
20.79	0.04	0.28	0.07	0.30	0.06	22.04	0.09	-0.31	0.12	0.00	0.18
20.79	0.04	-0.10	0.05	0.10	0.06	22.04	0.08	-0.12	0.11	-0.02	0.14
20.80	0.03	0.25	0.05	0.33	0.05	22.07	0.10	-0.21	0.13	0.24	0.18
20.80	0.04	-0.04	0.05	0.12	0.07	22.09	0.12	-0.12	0.15	-0.04	0.22
20.83	0.04	0.59	0.06	0.52	0.05	22.09	0.11	-0.33	0.13	-0.02	0.21
20.84	0.04	0.38	0.06	0.03	0.07	22.09	0.10	-0.50	0.12	0.14	0.16
20.85	0.04	0.40	0.07	0.50	0.06	22.12	0.10	0.03	0.13	0.06	0.16
20.86	0.05	0.40	0.06	0.47	0.06	22.13	0.11	0.33	0.17	0.34	0.16
20.86	0.03	-0.15	0.05	0.03	0.06	22.14	0.12	0.04	0.16	0.31	0.17
20.86	0.05	-0.43	0.07	0.07	0.08	22.16	0.11	-0.15	0.14	-0.06	0.23
20.87	0.04	0.03	0.06	0.10	0.06	22.19	0.12	0.39	0.17	0.19	0.20
20.87	0.04	-0.24	0.05	0.13	0.06	22.21	0.11	0.06	0.15	0.07	0.20
20.89	0.04	0.08	0.06	0.37	0.06	22.21	0.11	-0.38	0.14	0.00	0.21
20.91	0.03	-0.07	0.05	0.18	0.06	22.28	0.14	1.14	0.24	0.55	0.17
20.92	0.05	-0.01	0.07	0.02	0.08	22.33	0.12	0.03	0.15	0.42	0.16
20.92	0.04	0.43	0.08	0.40	0.06	22.33	0.11	-0.38	0.14	0.10	0.16
20.96	0.06	-0.42	0.07	0.25	0.09	22.33	0.12	0.08	0.16	0.23	0.20
20.99	0.04	-0.39	0.06	0.07	0.07	22.35	0.12	-0.18	0.16	0.32	0.17
20.99	0.05	0.81	0.09	0.54	0.07	22.38	0.13	0.07	0.17	0.45	0.17
21.00	0.05	1.11	0.11	0.57	0.06	22.40	0.11	0.76	0.22	0.85	0.13
21.01	0.05	0.45	0.07	0.43	0.07	22.40	0.13	-0.16	0.18	0.36	0.18
21.02	0.04	-0.15	0.05	0.11	0.07	22.42	0.13	-0.39	0.16	0.34	0.17
21.02	0.05	0.04	0.06	0.04	0.11	22.46	0.13	-0.09	0.17	0.24	0.20
21.03	0.04	-0.12	0.05	0.23	0.06	22.46	0.15	-0.26	0.17	0.39	0.19
21.03	0.04	-0.14	0.05	0.07	0.07	22.49	0.12	-0.15	0.17	-0.08	0.25
21.04	0.05	-0.34	0.07	0.10	0.08	22.52	0.18	-0.03	0.23	0.13	0.29
21.05	0.03	-0.08	0.06	0.12	0.07	22.53	0.13	-0.30	0.17	0.44	0.18
21.05	0.04	0.25	0.07	0.25	0.07	22.64	0.17	-0.45	0.20	0.35	0.23
21.07	0.06	0.07	0.09	-0.06	0.11	22.65	0.15	-0.37	0.18	0.22	0.23
21.07	0.05	1.89	0.16	0.91	0.06	22.67	0.17	-0.29	0.22	0.17	0.25
21.10	0.05	-0.21	0.06	0.15	0.07	22.69	0.15	-0.29	0.20	0.26	0.25
21.10	0.05	0.19	0.06	0.39	0.06	22.75	0.15	-0.44	0.19	0.32	0.23
21.12	0.05	0.39	0.08	0.47	0.09	22.93	0.21	-0.68	0.24	0.10	0.33
21.12	0.05	-0.13	0.06	0.22	0.07	23.07	0.25	-0.47	0.29	0.72	0.28
21.12	0.05	-0.39	0.06	0.03	0.09	23.09	0.23	-0.97	0.25	0.32	0.33

II. To consider the field star contamination toward Holmberg II, we assigned two ellipse regions as in Figure 1. The outer ellipse has $7'.9$ and $6'.3$ diameters of major and minor axes, and the inner ellipse has half size of the axes. Marks in Figures 2 and 3 indicate all stars detected in the observed field. Open circles represent stars located between the outer and inner ellipses, and filled circles are stars located inside the inner ellipse. It is apparent in Figures 2 and 3 that most of brightest stars having $V \approx 14 \sim 20$ and $R \approx 13 \sim 19$ are field stars located at the outside of the outer ellipse. Among the rest of stars with open and closed circles, many brightest stars located between the inner and outer ellipses would also be foreground field stars. Star count model of Ratnatunga & Bahcall (1985) predicts $\sim$ 20 Galactic foreground stars in the selected field of Figure 1 in the magnitude

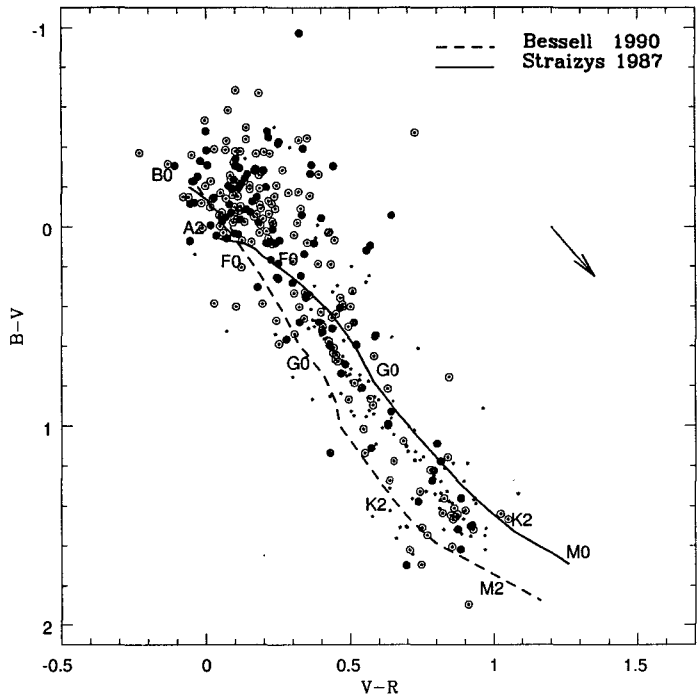

Figure 4. Color-color diagram of stars in Holmberg II. The loci with the solid and dotted lines present the colors of the Galactic supergiant stars (Straizys 1987, Bessell 1990). Symbols are the same as Figure 2.

range $17 - 20$ in V. We also note that the bright objects with $V \leq 18.4$ could be star clusters in Holmberg II or foreground stars, considering the upper limit of supergiant stars, i.e. $M_V = -9$ (Humphreyss 1983) and the distance modulus of Holmberg II.

To investigate the evolutionary status of the resolved stars, the theoretical evolution tracks of Salasnich et al. (2000) have compared with the observed CMDs. To transform the models into the observational planes, we performed the linear interpolation to the Lejeune et al. (1997) color transformation table. We also assumed a distance modulus of $\mu_o = 27.65$, extinctions of $A_B = 0.139, A_V = 0.107, A_R = 0.086$ (Schlegel et al. 1998), and a metallicity of $Z = 0.008$ (Stewart et al. 2000). It is apparent in Figures 2 and 3 that the majority of bright stars resolved in Holmberg II has initial mass between $\sim 10M_\odot$ and $20M_\odot$. This is in good agreement with the result of Hoessel & Danielson (1984), in which large number of supergiant stars with $9 \sim 25M_\odot$ were detected in the $(G-R, G)$ CMD. A few hot blue stars with initial masses over $20M_\odot$ are also present in $(B-V, V)$ CMD of Figure 2. This is also consistent with previous studies which suggest that recent massive star formation has occurred in Holmberg II (Hoessel & Danielson 1984, Stewart et al. 2000).

Figure 4 represents the $(V-R, B-V)$ color-color diagram for the resolved supergiant stars in Holmberg II with the loci defined by their Galactic counterparts. The solid and dashed lines are the loci for the Galactic supergiant stars given by Straizys (1987) and Bessell (1990), respectively. The

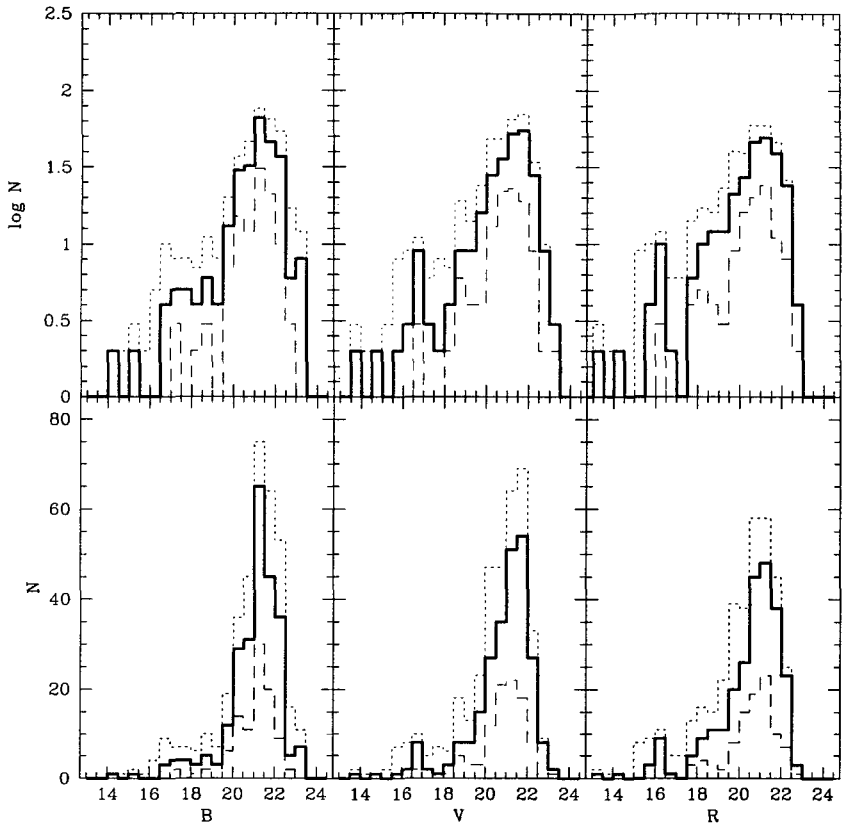

Figure 5. Luminosity functions of stars in Holmberg II. The dotted line indicates the luminosity function of stars detected in all observed field. The solid and dashed lines are those of stars located in the outer and inner ellipses.

dots, open and filled circles are same as Figures 2 and 3. It is evident that the Galactic foreground stars contribute to the scatter in the color-color diagram as in CMDs. The arrow in Figure 4 indicates five times of reddening vector, which implies that the effects of reddening are small in the observed field. Considering the Galactic supergiant sequence, we conclude that most of the observed stars in the color-color diagram are supergiant stars with a wide range of spectral type B-K.

3.3 LUMINOSITY FUNCTION

The luminosity function of the brightest stars in a galaxy provides a direct means of comparing the recent star formation condition with the other galaxies. The luminosity functions in B, V and R for all observed supergiant stars in the area of Holmberg II are plotted in Figure 5. While the dotted line indicates the luminosity function of stars detected in all observed field, the solid and dashed lines are those of stars located within the outer and inner ellipses as in Figure 1. Considering the

remained foreground field star contaminations, the bright ends of the logarithmic luminosity function are likely to follow power laws. The exponents have been determined by performing a least square fit to the logarithmic luminosity function of the outer ellipse with the brightness interval where the detection completeness is still high. The exponents computed in this manner are 0.33 ± 0.07 in B, 0.36 ± 0.03 in V and 0.28 ± 0.02 in R, respectively. The exponent in V is consistent with those of massive stars in OB associations of the Large and Small Magellanic Clouds (Hill et al. 1994). This result is indicative to confirm the similar recent star formation condition in the galaxies having similar morphology.

4. SUMMARY

We use B, V and R CCD images of Holmberg II to investigate the photometric properties of resolved supergiant stars. Total 374 stars are detected in all BVR band images of the observed field. Theoretical evolution tracks overlapped in the observed CMDs indicate that the supergiant stars in the observed field have progenitor masses between $\sim 10M_{\odot}$ and $20M_{\odot}$. A comparison the observed color-color diagram of the resolved stars with the Galactic supergiant sequence concludes that most of the observed stars in a color-color diagram are supergiant stars with spectral type B-K. The exponent of the logarithmic luminosity function in V of the resolved stars in Holmberg II is in good agreement with those of the Small and Large Magellanic Clouds.

ACKNOWLEDGEMENTS: Y.J.S. is grateful for the support by Korea Astronomy and Space Science Institute.

REFERENCES

Bessell, M. S. 1990, PASP, 102, 1181
de Vaucouleurs, G. 1964, AJ, 69, 737
Gallagher, J. S. & Wyse, R. F. G. 1994, PASP, 106, 1225
Grebel, E. K. 1998, Highlights Astron., 11, 125
Grebel, E. K. 2005, Stellar Astrophysics with the Worlds Largest Telescopes, AIP Conf. Proc. Vol. 752, eds. J. Mikolaewska & A. Olech (New York: AIP), p.161
Grebel, E. K. & Brandner, W. 1999, in New Views of the Magellanic Clouds, IAU Symp. Vol.190, eds. Y.-H. Chu, N. Suntzeff, J. Hesser, & D. Bohlender (San Francisco: ASP), p.470
Hill, R. J., Madore, B. F., & Freedman, W. L. 1994, ApJ, 429, 204
Hoessel, J. G. & Danielson, G. E. 1984, ApJ, 286, 159
Hoessel, J. G., Saha, A., & Danielson, G. E. 1998, AJ, 115, 573
Humphreys, R. M. 1983, ApJ, 269, 335
Kim, S., Staveley-Smith, L., Dopita, M. A., Freeman, K. C., Sault, R. J., Kesteven, M. J., & McConnell, D. 1998, ApJ, 503, 674
Landolt, A. U. 1992, AJ, 104, 372
Lejeune, Th., Cuisinier, F., & Buser, R. 1997, A&AS, 125, 229
Puche, D., Westpfahl, D., Brinks, E., & Roy, J. 1992, AJ, 103, 1841
Ratnatunga, K. U. & Bahcall, J. N. 1985, ApJS, 59, 63
Rozanski, R. & Rowan-Robinson, M. 1994, MNRAS, 271, 530
Salasnich, B., Girardi, L., Weiss, A., & Chiosi, C. 2000, A&A, 361, 1023
Schlegel, D. J., Finkbeiner, D. P., & Marc, D. 1998, ApJ, 500, 525
Sohn, Y. J. & Davidge, T. J. 1996a, AJ, 111, 2280

Sohn, Y. J. & Davidge, T. J. 1996b, AJ, 112, 2559
Sohn, Y. J. & Davidge, T. J. 1998, AJ, 115, 130
Staveley-Smith, L., Sault, R. J., Hatzidimitriou, D., Kesteven, M. J., & McConnell, D. 1997, MNRAS, 289, 225
Stetson, P. B. 1987, PASP, 99, 191
Stetson, P. B. & Harris, W. E. 1988, AJ, 96, 909
Stewart, S. G., Fanelli, M. N., Byrd, G. G., Hill, J. K., Westpfahl, D. J., Cheng, K.-P., O'Connel, R W., Rorberts, M. S., Neff, S. G., Smith, A. M., & Stecher, T. P. 2000, ApJ, 529, 201
Straizys, V. 1987, Bull. Vilnius Observ., 78, 43
Tolstoy, E. 2003, AP&SS, 284, 579
van den Bergh, S. 1999, A&ARv, 9, 273